

Numerical investigation of strong-field photoionization rates

 Jarosław H. Bauer^{1,*} and Jacek Matulewski²
¹*Katedra Fizyki Teoretycznej Uniwersytetu Łódzkiego, Ul. Pomorska 149/153, PL-90–236 Łódź, Poland*
²*Instytut Fizyki, Uniwersytet Mikołaja Kopernika, Ul. Grudziądzka 5, PL-87–100 Toruń, Poland*

(Received 31 May 2010; revised manuscript received 26 July 2010; published 29 November 2010)

The time-dependent Schrödinger equation for a two-dimensional model atom is solved exactly (numerically) for pulses of a circularly or linearly polarized strong laser field (in the dipole approximation). Although exact final ionization (or survival) probabilities do not depend on the choice of gauge, we show (both analytically and numerically) that ionization rates, calculated for a flat part of the strong laser pulse, may be gauge dependent. Differences between the length gauge and the velocity gauge ionization rates or survival probabilities (calculated through projections on “textbook” bound states) usually grow with an intensity of the laser field. The differences, which vanish in the limit of a weak field, may reach even a factor of 4 to the advantage of the length gauge for stronger fields. This fact points out that such a method of computing ionization rates may be not reliable in strong laser fields. Gauge-invariant ionization rates, calculated through a probability of finding an electron in a vicinity of a nucleus, usually have values being found between values of the previously mentioned gauge-dependent ionization rates.

 DOI: [10.1103/PhysRevA.82.053418](https://doi.org/10.1103/PhysRevA.82.053418)

PACS number(s): 32.80.Rm, 33.20.Xx, 33.60.+q, 33.80.–b

I. INTRODUCTION

Usually either of two forms of the Hamiltonian, describing an interaction of an initially bound electron with strong laser fields (e.g., Refs. [1] (pp. 315–328) and [2–10]), appears in problems concerning photoionization (or photodetachment). These Hamiltonian forms are the length gauge (LG) one $H_I^{dE} = \vec{r}\vec{F}(t)$ and the velocity gauge (VG) one $H_I^{pA} = \vec{A}(t)\hat{p}/c + \vec{A}(t)^2/2c^2$, respectively ($\hat{p} = -i\vec{\nabla}$; in what follows we use atomic units $\hbar = e = m_e = 1$, substituting explicitly -1 for the electronic charge). The fact that both the electric field vector $\vec{F}(t)$ and the vector potential $\vec{A}(t)$ of the laser field [connected by the relation $\vec{F}(t) = -c^{-1}(\partial\vec{A}/\partial t)$] depend only on time means that the dipole approximation has been applied. In the present work we disregard any nondipole or relativistic effects in the photoionization process. The approximation is fully justified for laser amplitudes E_0 lower than 20 a.u. and for the laser frequency $\omega = 1$ a.u. (as used in the whole paper).

The time-dependent Schrödinger equation (TDSE) for a real three-dimensional (3D) hydrogen atom is the following:

$$i\frac{\partial}{\partial t}\Psi(\vec{r},t) = H\Psi(\vec{r},t), \quad H = \frac{\hat{p}^2}{2} - \frac{Z}{r} + H_I = H_A + H_I, \quad (1)$$

where $Z = 1$, H_I is either in the LG or in the VG, and $H_A = \hat{p}^2/2 - Z/r$ is the atomic Hamiltonian. Let us assume that a total duration of the circularly polarized laser pulse is τ , $\vec{A}(0) = \vec{A}(\tau) = \vec{0}$, and the initial condition $\Psi(\vec{r},t=0) = \Phi_{100}(\vec{r})$ is obeyed in both gauges. $\Phi_{nlm}(\vec{r})$ denote the standard “textbook” stationary solutions to the Schrödinger equation (bound states), with the usual meaning of the (n,l,m) quantum numbers. The positive energy solutions to the same Schrödinger equation (continuum states) are parametrized by their asymptotic momentum \vec{p} . Both types of wave functions obey the well-known equations:

$$H_A\Phi_{nlm}(\vec{r}) = E_n\Phi_{nlm}(\vec{r}), \quad H_A\Phi_{\vec{p}}(\vec{r}) = E\Phi_{\vec{p}}(\vec{r}), \quad (2)$$

with $E_n = -1/2n^2 < 0$ and $E = p^2/2 > 0$. There is a well-known relation between exact solutions to the TDSE in both gauges:

$$\Psi^{dE}(\vec{r},t) = \hat{U}(\vec{r},t)\Psi^{pA}(\vec{r},t) = \exp\left(\frac{i}{c}\vec{r}\vec{A}(t)\right)\Psi^{pA}(\vec{r},t), \quad (3)$$

where $\hat{U}(\vec{r},t)$ is a unitary operator. Let us expand the two wave functions from Eq. (3) in a basis set (which is orthonormal and complete) of eigenstates of the atomic Hamiltonian H_A :

$$\Psi^{dE}(\vec{r},t) = \sum_{nlm} a_{nlm}(t)\phi_{nlm}(\vec{r}) + \int d^3p a_{\vec{p}}(t)\phi_{\vec{p}}(\vec{r}), \quad (4)$$

$$\Psi^{pA}(\vec{r},t) = \sum_{nlm} b_{nlm}(t)\phi_{nlm}(\vec{r}) + \int d^3p b_{\vec{p}}(t)\phi_{\vec{p}}(\vec{r}). \quad (5)$$

An exact numerical solution to the TDSE in the LG or in the VG is equivalent to a statement that all the time-dependent coefficients $a(t)$ and $b(t)$ are known. From orthonormality of the functions $\Phi(\vec{r})$ one obtains

$$1 = \int d^3r |\Psi^{dE}(\vec{r},t)|^2 = \sum_{nlm} |a_{nlm}(t)|^2 + \int d^3p |a_{\vec{p}}(t)|^2 \equiv p_{\text{bound}}(t) + p_{\text{free}}(t), \quad (6)$$

$$1 = \int d^3r |\Psi^{pA}(\vec{r},t)|^2 = \sum_{nlm} |b_{nlm}(t)|^2 + \int d^3p |b_{\vec{p}}(t)|^2 \equiv p'_{\text{bound}}(t) + p'_{\text{free}}(t). \quad (7)$$

Multiplying Eq. (5) by $\hat{U}(\vec{r},t)$, we obtain from Eq. (3),

$$\Psi^{dE}(\vec{r},t) = \sum_{nlm} b_{nlm}(t)\hat{U}(\vec{r},t)\Phi_{nlm}(\vec{r}) + \int d^3p b_{\vec{p}}(t)\hat{U}(\vec{r},t)\Phi_{\vec{p}}(\vec{r}). \quad (8)$$

Comparing Eqs. (4) and (8) one can see that both expansions of the wave function $\Psi^{dE}(\vec{r},t)$ are different for an arbitrary t , unless $\hat{U}(\vec{r},t) = 1$. The latter condition is fulfilled for an arbitrary \vec{r} only when $\vec{A}(t) = \vec{0}$. Then for all the functions of time $a_{nlm}(t) = b_{nlm}(t)$ and $a_{\vec{p}}(t) = b_{\vec{p}}(t)$. [Strictly speaking,

*bauer@uni.lodz.pl

when $\vec{F}(t) \neq \vec{0}$, such a situation is possible only for a linear polarization of the laser field, twice every laser cycle, and impossible for other ellipticities of the field.]

For the circular polarization, during the laser pulse $\vec{A}(t) \neq \vec{0}$ always (except two instants: $t = 0$ and $t = \tau$). Therefore, in general, one has $a_{nlm}(t) \neq b_{nlm}(t)$ and $a_{\vec{p}}(t) \neq b_{\vec{p}}(t)$. Moreover, the same holds also for absolute values (squared): $|a_{nlm}(t)|^2 \neq |b_{nlm}(t)|^2$ and $|a_{\vec{p}}(t)|^2 \neq |b_{\vec{p}}(t)|^2$. This is because $\hat{U}(\vec{r}, t) \neq 1$ and $\hat{U}(\vec{r}, t)$ does not factorize into functions depending only on \vec{r} and only on t . There is no simple relation between the coefficients $a(t)$ and $b(t)$ when the circularly polarized laser field is on. Furthermore, it appears that for settled specific parameters (n_0, l_0, m_0) or \vec{p}_0 the respective coefficients $b_{n_0 l_0 m_0}(t)$ or $b_{\vec{p}_0}(t)$ have to be expressed by the coefficients $a_{nlm}(t)$ and $a_{\vec{p}}(t)$, corresponding to all possible parameters (n, l, m) and \vec{p} . For example, when $(n_0, l_0, m_0) = (1, 0, 0)$ we obtain

$$b_{100}(t) = \sum_{nlm} a_{nlm}(t) \int d^3r \Phi_{100}^*(\vec{r}) \hat{U}^\dagger(\vec{r}, t) \Phi_{nlm}(\vec{r}) + \int d^3r p a_{\vec{p}}(t) \int d^3r \Phi_{100}^*(\vec{r}) \hat{U}^\dagger(\vec{r}, t) \Phi_{\vec{p}}(\vec{r}), \quad (9)$$

where $\hat{U}^\dagger(\vec{r}, t) = \exp(-i\vec{r}\vec{A}(t)/c)$. Analogous expressions for other coefficients $b_{nlm}(t)$ and for $b_{\vec{p}}(t)$ may be obtained easily from Eqs. (3)–(5). Of course, in a similar way, one can also obtain the reverse relations expressing a particular coefficient $a(t)$ by all existing coefficients $b(t)$. [Then, in a counterpart of Eq. (9), $\hat{U}^\dagger(\vec{r}, t)$ should be replaced by $\hat{U}(\vec{r}, t)$.]

II. DISCUSSION

Our considerations shown hitherto resemble those of Kobe and Wen [2], who studied the problem of gauge invariance for a one-dimensional (1D) harmonic oscillator in a strong electromagnetic field (but, in fact, they used the dipole approximation, too). For the particular problem considered by Kobe and Wen, unlike in our case, an exact analytical solution to the respective TDSE exists. The main conclusion of their work is the physical significance they attach to the counterparts of $a(t)$ [but not $b(t)$] for an arbitrary t for the harmonic oscillator. Similar conclusions about both types of expansion coefficients appear in the work of Lamb *et al.* [4] in the context of a two-level atom. However, Grobe and Fedorov [5] claim that “it is difficult to give a widely accepted definition of the photodetachment probability in the presence of the field.” According to Cormier and Lambropoulos [7], the VG is, in general, more adapted than the LG to a study of strong-field ionization for dynamical reasons, but “only the LG permits one to monitor the dynamics of the bare atom eigenstates during the illumination by the field.” The dynamics is connected with a notion of the ionization rate (probability per unit time), which is called in question for very strong fields by Geltman [6,11].

A realistic pulse envelope induces rapid changes in the bound-states population, especially during its turning on and off. Therefore, a process of the pulse switching on and off is truly hard for theoretical description. On the faith of a set of numerical simulation cases it is also very difficult to establish some basic rules allowing one to predict, for example, the pop-

ulation of bound states after the smooth switch-on of the laser. Moreover, it is important to note that this process may result in a significant transfer of the population to continuum states or even in its complete ionization [12]. The electron dynamics is much slower, when the laser field is constant (the plateau of the pulse). Furthermore, this part of the pulse is responsible for the most interesting effects of strong-field optics (e.g., for the adiabatic stabilization [13]). Thus many theories exist, which try to focus on this aspect of the whole process and somehow exclude the effect of the dynamical beginning and end of the laser-atom interaction (for instance, the Floquet-states theories). These approaches proved their effectiveness, despite their obvious simplifications. A characteristic feature of these theories is the assumption that a constant rate is sufficient to describe the laser-atom interaction for the given laser intensity and frequency, at least during the flat part of the pulse. Our numerical simulation also confirms such an assumption, if one limits himself to the time interval in which the laser field is constant. Of course, ignoring the laser switch-on and switch-off is not possible in the numerical simulations. The laser has to be somehow switched on. However, our aim is to try to marry both approaches, that is, to determine or refine the constant rates from time-dependent quantities calculated thanks to numerical simulations. Nevertheless, we are conscious of limits of such a trial.

Ionization rates were computed within the strong-field S -matrix theories (also known as the strong-field approximation) by one of us (J.H.B.) [8–10] both in the LG and in the VG. One of the main conclusions one can draw from these works is that for sufficiently strong laser fields, differences between both gauges grow with increasing intensity of the laser field (see, e.g., Fig. 5 in Ref. [8], Figs. 1 and 2 in Ref. [9], Figs. 1–4 and 10 in Ref. [10]). In Fig. 1 we show the VG and LG ionization rates as a function of intensity of the circularly polarized laser field for the $H(1s)$ atom (in fact, this is Fig. 1 from Ref. [10]). Ionization rates, shown in Fig. 1, were computed using the S -matrix theory in the version of Keldysh [14] (LG, solid lines) and in the version of Reiss [15] (VG, dotted lines). Moreover, for some initial states of the hydrogen atom, and the circularly polarized laser field, qualitative

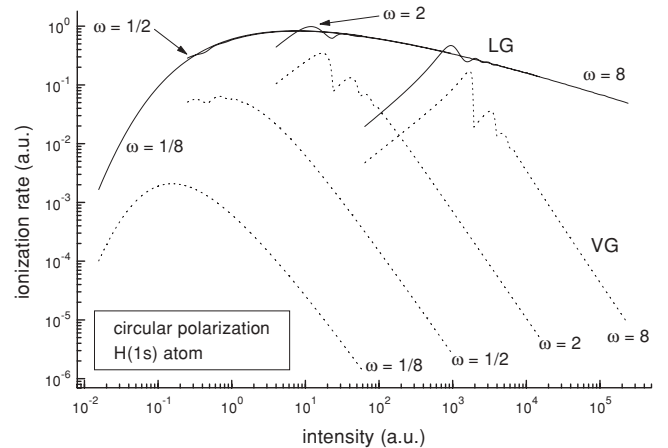


FIG. 1. The VG and LG S -matrix ionization rates of the $H(1s)$ atom in the circularly polarized laser field for $\omega = 1/8, 1/2, 2,$ and 8 a.u. versus intensity of the laser field.

differences in the spectra of ionized photoelectrons appear (see Figs. 5–8 and 13 in Ref. [10]). These differences deepen with increasing the field. In principle, the calculations [8–10] should be more accurate, as the field becomes stronger. But two dispersing results cannot, of course, converge to the same exact result at the same time (in the limit of a very intense laser field, for constant laser frequency). Also the reasoning presented here in Sec. I, Eq. (9), and analogous expressions for other coefficients $b(t)$ indicate that differences between both gauges might grow with increasing field, because $\hat{U}^\dagger(\vec{r}, t)$ deviates from unity as $\vec{A}(t)$ increases. Furthermore, it seems reasonable to ask what are really exact ionization rates in both gauges for strong laser fields of constant frequency and intensity, using accurate solutions to the TDSE, and this is the main aim of our present work. Equations (6) and (7) define probabilities of finding the electron in either bound or free states [$p_{\text{bound}}(t)$ or $p_{\text{free}}(t)$] of the hydrogen atom when the laser field is on. (More precisely, bound or free states denote here the “textbook” wave functions without any additional phase factors.) Let us notice that, in the S -matrix theory, the exact probability amplitude of ionization is defined through projecting the exact solution to the TDSE $\Psi_f^{(-)}$ (for example, in the LG) on the “textbook” ground state Φ_i :

$$\begin{aligned}
 (S - 1)_{fi} &= S_{fi} - \delta_{fi} = \lim_{t \rightarrow -\infty} (\Psi_f^{(-)}, \Phi_i) \\
 &\quad - \lim_{t \rightarrow +\infty} (\Psi_f^{(-)}, \Phi_i) = \int_{-\infty}^{+\infty} dt \frac{\partial}{\partial t} (\Psi_f^{(-)}, \Phi_i) \\
 &= - \int_{-\infty}^{+\infty} dt \left(\frac{\partial}{\partial t} \Psi_f^{(-)}, \Phi_i \right) \\
 &\quad - \int_{-\infty}^{+\infty} dt \left(\Psi_f^{(-)}, \frac{\partial}{\partial t} \Phi_i \right) \\
 &= - \int_{-\infty}^{+\infty} dt \left(\frac{1}{i} (H_A + H_I) \Psi_f^{(-)}, \Phi_i \right) \\
 &\quad - \int_{-\infty}^{+\infty} dt \left(\Psi_f^{(-)}, \frac{1}{i} H_A \Phi_i \right) \\
 &= -i \int_{-\infty}^{+\infty} dt (\Psi_f^{(-)}, H_I \Phi_i), \tag{10}
 \end{aligned}$$

(for next steps of this theory and more detail see Refs. [15] and [9]). Let us remember that the S -matrix theory ignores ionization during the rise and fall of the laser pulse, where one assumes that $\vec{A}(t)$ is switched on and off adiabatically. Therefore, in the present work, we are only interested in exact (numerical) calculation of the ionization rate for the flat top of the laser pulse.

In the following, in Eq. (11), using Eqs. (6) and (7), we write down a pair of expressions describing instantaneous ionization rates both in the LG [$\Gamma_{\text{LG}}(t)$] and in the VG [$\Gamma_{\text{VG}}(t)$], respectively,

$$p_{\text{free}}(t) = 1 - \sum_{nlm} |a_{nlm}(t)|^2, \quad p'_{\text{free}}(t) = 1 - \sum_{nlm} |b_{nlm}(t)|^2, \tag{11a}$$

$$\begin{aligned}
 p_{\text{free}}(t) &= 1 - \exp \left[- \int_0^t \Gamma_{\text{LG}}(t') dt' \right], \quad p'_{\text{free}}(t) = 1 \\
 &\quad - \exp \left[- \int_0^t \Gamma_{\text{VG}}(t') dt' \right]. \tag{11b}
 \end{aligned}$$

In Eq. (11b) depletion effects (of an initial state) are taken into account. The quantities $\Gamma_{\text{LG}}(t)$ and $\Gamma_{\text{VG}}(t)$ may oscillate periodically (as Figs. 2 and 3 clearly show), so we are concerned with ionization rates averaged over a cycle of the field. Bauer and Ceccherini [16] and Boca *et al.* [17] computed, among other things, ionization rates for the $H(1s)$ atom in the strong circularly polarized laser field for $\omega = 1$ a.u. and $\omega = 2$ a.u. with the help of numerical solutions to the TDSE. According to the authors of Refs. [16,17], their results are accurate and they do not mention any problem with the choice of gauge. However, it follows from mathematical formulas given in Refs. [16] and [17] that these ionization rates were computed in the VG. For example, on p. 152, after Fig. 3 in Ref. [17] there is the following statement: “Our TDSE rates were obtained by following in time the decay of the projection of the wavefunction Ψ on the field-free $1s$ state (specifically $|(1s | \Psi)|^2$) during the flat top of an adiabatically turned-on pulse.” In our notation, this means that it is $|b_{100}(t)|^2$, which was calculated in Ref. [17].

III. METHOD AND RESULTS

For both weak and strong (but not superstrong) laser fields ionized electrons are mostly emitted in the polarization plane. This is a result of validity of the dipole approximation, and an absence of magnetic-field effects in the plane-wave field. Therefore, in the present work, we solve the TDSE, Eq. (1), in a two-dimensional (2D) instead of a three-dimensional (3D) space. We do not expect any qualitative differences between 2D and 3D for strong-field ionization rates, as our experience shows (for example, cf. Figs. 1 and 10 in Ref. [10]). We also note that analogous 3D data in Ref. [16] (in the VG) are close to 2D data of the present work (see Tables I, III, IV, and the VG). The evolution of the wave packet in 2D is calculated using the alternate-direction implicit algorithm (ADI) for Hamiltonian in the VG. To cover the space range of the wave-packet oscillations in the circular, as well as in the linear polarization, the spatial grid size is equal to $(-50:50)$ in both directions with the spatial step equal to about 0.1 (1024 nodes in every direction). The negative imaginary potential has been set at the edges of the grid in order to absorb the outgoing parts of the wave packet [18]. A time step is equal to $T/1000$, where T is the field period $T = 2\pi/\omega$. The laser frequency $\omega = 1$ a.u. is kept constant throughout this work. The convergences of the results for spatial nodes density, the spatial grid extent, and the time step have been checked. Time-dependent quantities (e.g., the populations of bound states) are calculated in each time step in two variants: involving the unitary transformation \hat{U} (which assures that obtained results are identical to those calculated in the LG) and omitting it (i.e., using a so-called mixed gauge [19]), which corresponds to the VG. Then the sum of 22 bound states with the lowest energies is calculated. There are two methods, which were often used to find (exact or approximate) ionization rates in nonperturbative laser fields. One can either consider (A) the projection of $\Psi(\vec{r}, t)$ [obeying Eq. (1)] on “textbook” bound states, or one can consider (B) the norm of $\Psi(\vec{r}, t)$ in a large finite volume with boundaries well removed from the origin. Equation (11) corresponds to the method (A), and Eq. (15) corresponds to the method (B). Since both methods are very different from the very nature of

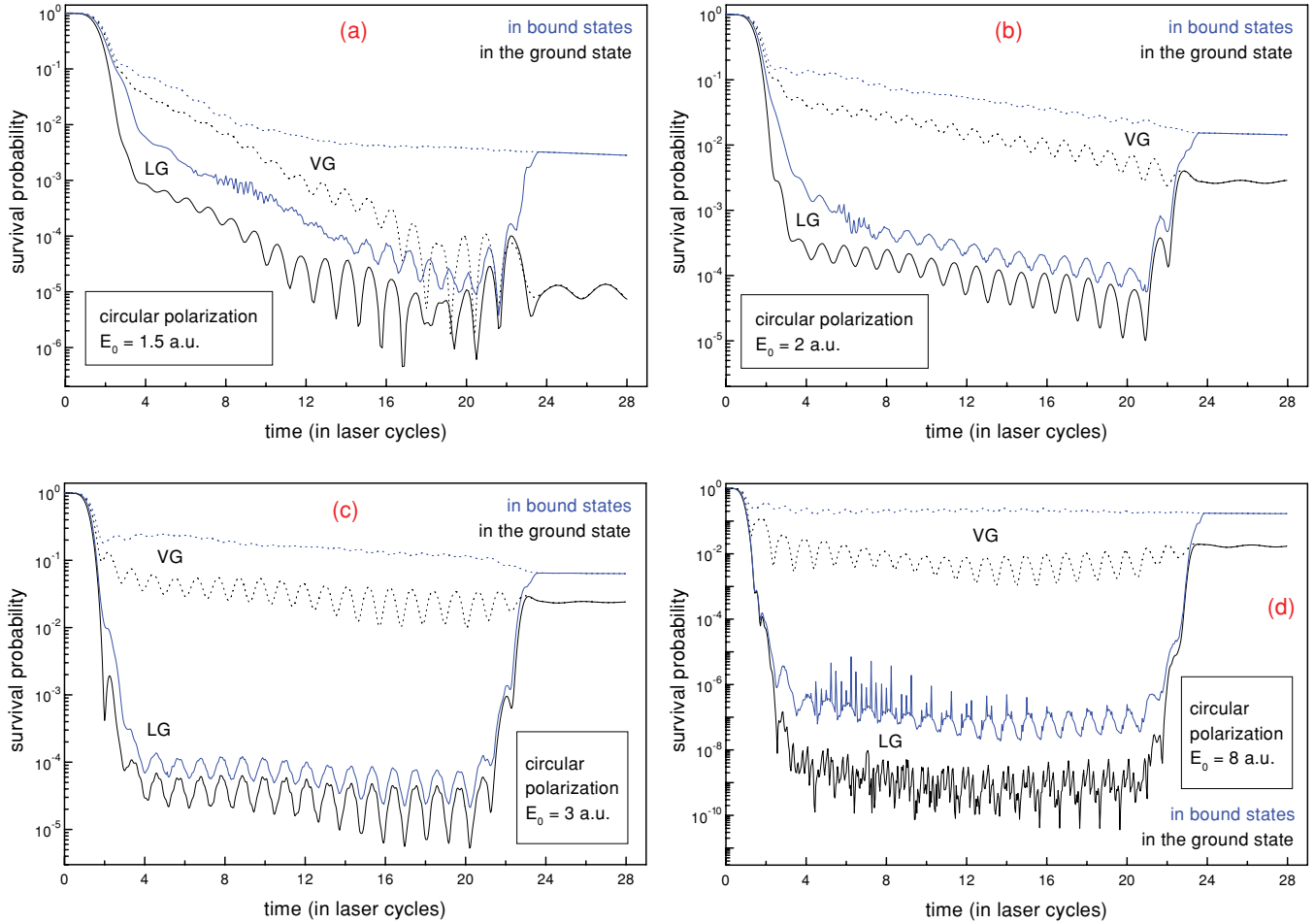


FIG. 2. (Color online) Survival probability versus time for a trapezoidal circularly polarized laser pulse of the frequency $\omega = 1$ a.u.. The turn-on and turn-off times of the pulse are equal to four cycles. The flat part of the pulse is for $4 \leq t \leq 20$ (in laser cycles). LG stands for the length gauge and VG for the velocity gauge. In the consecutive plots (a)–(d) the electric field vector amplitude E_0 increases, as shown on graphs (see text for more detail).

things, we will call the method (A) the bound states projection method (BSPM).

In our numerical calculations we apply the field parameters identical to those from Fig. 1 in Ref. [16]. The laser pulse has a trapezoidal envelope (for the electric field vector) $4T - 16T - 4T$ in all simulations presented in this paper. We solve the TDSE with the initial condition $\Psi^{dE}(\vec{r}, t=0) = \Psi^{pA}(\vec{r}, t=0) = \Phi_{\text{ground}}(\vec{r})$, where the initial ground-state wave function is given by

$$\Phi_{\text{ground}}(\vec{r}) = \frac{4Z}{\sqrt{2\pi}} \exp(-2Zr), \quad (12)$$

and is normalized to unity in an entire space. We put $Z = 0.5$, because this value in 2D gives the same binding energy $E_B = 2Z^2 = 0.5$ a.u. as for the real 3D $H(1s)$ atom. In Figs. 2(a)–2(d) we show survival probabilities versus time during the circularly polarized laser pulse, both in all bound states (colored or gray lines) and in the ground state (black lines) of our 2D model atom. Consecutive plots (a)–(d) correspond to $E_0 = 1.5, 2, 3,$ and 8 a.u., where E_0 is the peak electric field during the flat part of the pulse. The LG probabilities are shown by solid lines, and the VG ones by dotted lines. The respective LG and VG curves

merge at $t = 0$ and $t = 24T$, because then $\vec{A}(t) = \vec{0}$. [Also for $24T < t \leq 28T$ $\vec{A}(t) = \vec{0}$.] Figures 2(a)–2(d) show that during the pulse, populations of bound states in the VG are always greater than in the LG, particularly in the flat part of the pulse (for $4T \leq t \leq 20T$). Differences between both gauges grow rapidly, up to several orders of magnitude, with increasing E_0 . In Figs. 2(a)–2(d) one can observe decays of bound states for $4T \leq t \leq 20T$. A purely exponential decay,

$$p(t) = p_0 \exp(-\Gamma t), \quad (13)$$

would be a straight line with a negative slope in Fig. 2. Neglecting oscillations, one can indeed observe roughly exponential decays, particularly well visible in all the curves from Figs. 2(b) and 2(c). Nevertheless, we have computed numerically the average BSPM ionization rates in both gauges, assuming approximate validity of Eq. (13) for $4T \leq t \leq 20T$, taking into account all important bound states (22 ones with the lowest energies). This has been done for four different values of E_0 from Fig. 2 and also for two greater values of E_0 . The results, which are given in Table I, have been obtained by the least-square method at the level of confidence

TABLE I. The BSPM ionization rates (in both gauges) for the circularly polarized laser field as a function of the electric field vector amplitude E_0 . The data have been obtained by the least-square method at the confidence level of 95%. Shown also is the ratio of both results. $2.79 \pm 0.02[-2]$ denotes $(2.79 \pm 0.02) \times 10^{-2}$.

E_0 (a.u.)	Γ_{VG} (a.u.)	Γ_{LG} (a.u.)	$\Gamma_{\text{LG}}/\Gamma_{\text{VG}}$
1.5	$2.79 \pm 0.02[-2]$	$6.03 \pm 0.14[-2]$	2.16
2	$1.717 \pm 0.003[-2]$	$2.49 \pm 0.14[-2]$	1.45
3	$7.80 \pm 0.02[-3]$	$8.31 \pm 0.18[-3]$	1.07
8	$-3.2 \pm 0.5[-4]^a$	$1.68 \pm 0.04[-2]$	—
13	$8.52 \pm 0.12[-3]$	$3.50 \pm 0.08[-2]$	4.11
18	$1.160 \pm 0.018[-2]$	$4.44 \pm 0.08[-2]$	3.83

^aIn the interval $[4T, 12T]$ $\Gamma_{\text{VG}} = -2.82 \pm 0.14[-3]$, and in the interval $[12T, 20T]$ $\Gamma_{\text{VG}} = 2.52 \pm 0.11[-3]$.

equal to 95% (for 16 000 points belonging to the time interval $[4T, 20T]$ and two parameters of the searched line). This method, which we trust most, gives the BSPM ionization rates with their uncertainties (see Table I). In the appendix we give the BSPM ionization rates, corresponding to the same values of E_0 , computed with the help of two other methods (see Tables III and IV). The data from these tables show that the BSPM ionization rates are different in both gauges and the LG ones (Γ_{LG}) are usually greater than the VG ones (Γ_{VG}). It follows from Figs. 2(a)–2(d) that if one knows the VG survival probability at $t = 4T$ (an onset of the flat part of the pulse) and Γ_{VG} , one can approximately compute the final gauge-invariant survival probability at the end of the pulse. As a matter of fact, this remark is in agreement with the discussion of Grobe and Fedorov (in Sec. 6 of Ref. [5]) in a context of the strong-field photodetachment investigated numerically in the 1D model. On the other hand, it would not be possible to make similar predictions in the LG, as Figs. 2(a)–2(d) clearly show, because for $20T \leq t \leq 24T$ survival probabilities in bound states (unlike in the VG) grow rapidly. The LG probabilities at time t represent the electron “as if the field were switched off abruptly at time t ” [5]. Such an abrupt switch-off, for $4T \leq t \leq 20T$, would leave the electronic wave packet quite far from the origin, where overlaps with bound states are very small. In contrast, the VG probabilities at time t give an “information about the residual bound state probability after the end of the pulse as if the pulse ended at time t ” [provided that $\vec{A}(t)$ is zero at the end of the pulse] [5]. Therefore, the VG probabilities at time t correspond to a smooth switch-off of the pulse and usually much smaller excursion amplitude of the electron (and much larger overlap with bound states).

Let us note that our numerical values of Γ_{VG} for $E_0 = 1.5, 2$, and 3 a.u. (from Tables I, III, and IV) are quite close to those from Fig. 3(a) in Ref. [16]. This means that for the circularly polarized laser field, and for the physical quantities considered here, our simplified 2D model atom gives a reasonable approximation to the real (3D) atom. We have also made similar calculations for the same pulse and the linear polarization. In this case survival probabilities oscillate much more rapidly within one laser cycle, particularly in the LG. Figures 3(a) and 3(b) show results for $E_0 = 2$ a.u.. Likewise, Figs. 3(c) and 3(d) show results for $E_0 =$

8 a.u.. (The lines in Fig. 3 are marked in a way similar to Fig. 2.) For the linear polarization the VG populations in bound states coincide with the LG ones whenever $\vec{A}(t) \equiv \vec{0}$, but may differ by a few orders of magnitude when $\vec{A}(t)$ achieves a local maximum. Let us look at all bound states (in the VG) in Figs. 3(a) and 3(c) for $4T \leq t \leq 20T$. One can conclude that the final gauge-invariant survival probabilities at the end of the pulse could be approximately predicted, if one knows the VG survival probability at $t = 4T$ and Γ_{VG} . Therefore, this feature of the VG seems to be independent on the laser field polarization. Again, like for the circular polarization, such a prediction would be very difficult in the LG [see Figs. 3(b) and 3(d)]. Of course, we note that Γ_{VG} (averaged over a field period) is not constant for $4T \leq t \leq 20T$ in Figs. 2(a), 2(d), and 3(a) (for more detail see the appendix).

The instantaneous BSPM ionization rates, defined by Eqs. (6), (7), and (11), in general may be gauge dependent. As we have shown earlier, the average BSPM ionization rates (for an integer number of laser cycles) may also be gauge dependent for the flat part of the laser pulse. From Eq. (3) and the condition $\vec{A}(\tau) = \vec{0}$ one obtains

$$\Psi^{dE}(\vec{r}, \tau) = \exp\left(\frac{i}{c}\vec{r}\vec{A}(\tau)\right)\Psi^{pA}(\vec{r}, \tau) = \Psi^{pA}(\vec{r}, \tau). \quad (14)$$

As a result, at the end of the pulse ($t = \tau$) the LG and the VG survival probabilities (in any bound state) have to be equal. This fact is not in a contradiction with the differences between Γ_{VG} and Γ_{LG} from Tables I, III, and IV, because both Γ_{VG} and Γ_{LG} have been calculated only for $4T \leq t \leq 20T$. There are the nonzero BSPM ionization rates for $0 \leq t \leq 4T$ and for $20T \leq t \leq 24T$, which also contribute to gauge-invariant final ionization probabilities. There are two elements which have an effect on survival probabilities shown in Fig. 2. The first one is connected with an irreversible depletion of the bound-states population due to the laser field, and only this element plays a part at the flat top of the pulse. But there is another element, which is connected with a considerable change of a position of the electronic wave packet in space. Roughly speaking, the classical displacement from the origin (called also the excursion amplitude) changes from E_0/ω^2 to zero when time increases from $t = 20T$ to $t = 24T$. As a result, the overlap of the electronic wave packet with the ground state (but also with other bound states) grows significantly. Therefore, in this time interval, the second element prevails over the first one.

To avoid problems with the gauge-dependent BSPM ionization rates one can use another measure of the ionization rate. Namely, one can define the instantaneous ionization rate $\Gamma(t)$ through the following relations:

$$p_{\text{ion}}(t) = 1 - N(t) = 1 - \iint_{\text{grid}} dx dy |\Psi(x, y, t)|^2, \quad (15a)$$

$$p_{\text{ion}}(t) = 1 - \exp\left[-\int_0^t \Gamma(t') dt'\right], \quad (15b)$$

where $N(t)$ denotes a probability of finding the electron in the vicinity of the nucleus, and where the wave function $\Psi(x, y, t)$ is the exact solution to the TDSE [Eq. (1)]. The earlier integration extends over the entire 2D space covered by

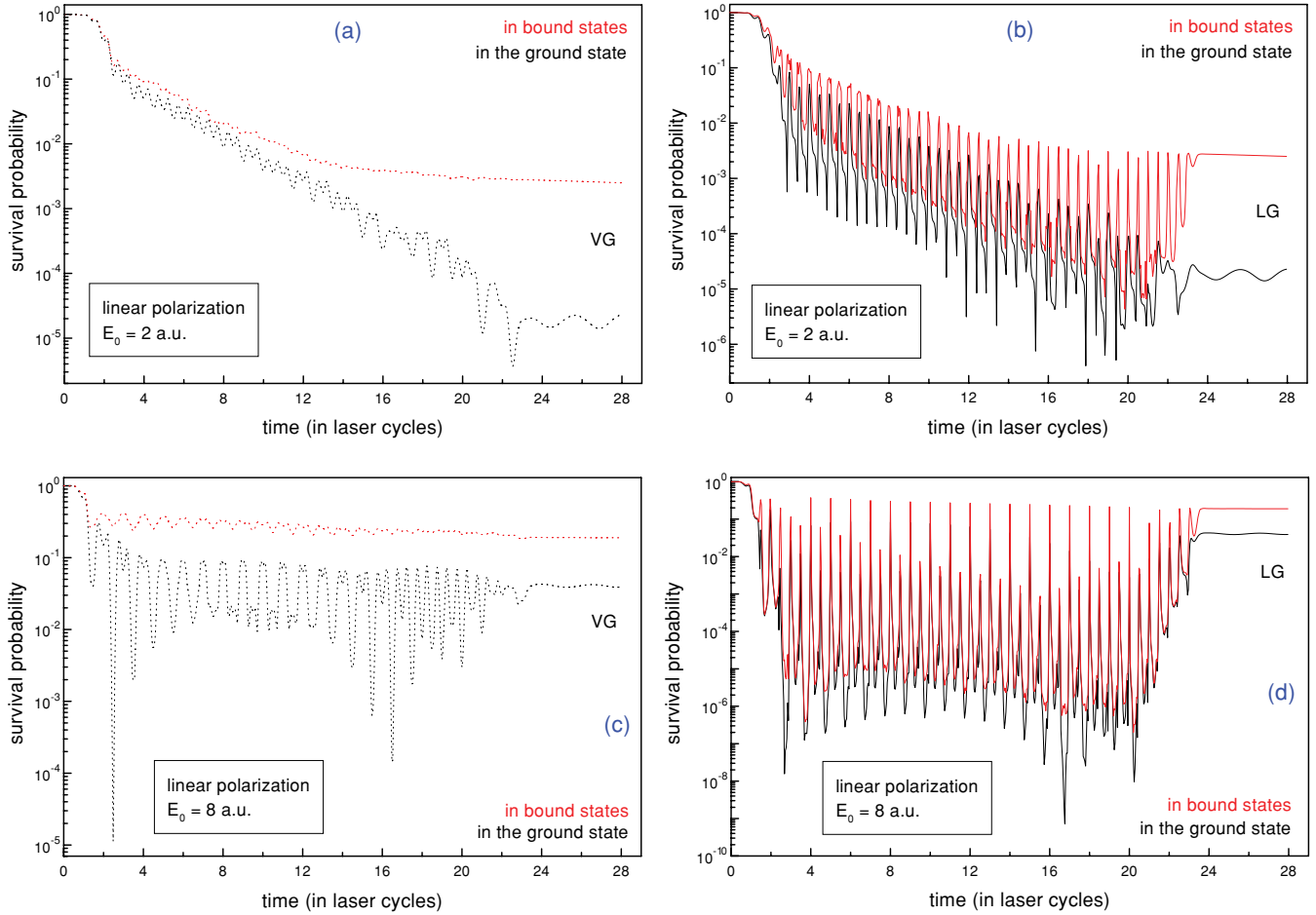


FIG. 3. (Color online) Survival probability versus time for a trapezoidal linearly polarized laser pulse of the frequency $\omega = 1$ a.u.. The turn-on and turn-off times of the pulse are equal to four cycles. The flat part of the pulse is for $4 \leq t \leq 20$ (in laser cycles). LG stands for the length gauge and VG for the velocity gauge. In plots (a) and (b) the electric field vector amplitude $E_0 = 2$ a.u.; in plots (c) and (d) $E_0 = 8$ a.u. (see text for more detail).

the grid (in our case, from -50 to 50 a.u. in both directions). We assume that limits of integration in Eq. (15a) are far enough from the excursion amplitude of the ionized electron ($E_0/\omega^2 = E_0 \leq 18$ a.u.). In Eq. (15b) depletion effects [like in Eq. (11b)] are taken into account. It follows from Eq. (3) that $\Gamma(t)$ from Eq. (15b) is gauge invariant. However, the drawback of the definition from Eq. (15) is that the atom “ionizes” also after the switch-off of the laser field, because the probability $N(t)$ decreases for $t > 24T$. There is always a certain time delay between a real ionization and the ionization displayed by the functions $N(t)$ and $\Gamma(t)$, because the ionized part of the electronic wave packet needs some time to leave the grid. This time delay, at least currently for us, is truly hard to evaluate.

In Fig. 4 we present the probability $N(t)$ as a function of time for six different simulations corresponding to the circular polarization and the same pulses as in Tables I–IV. As one could expect, the consecutive curves show roughly exponential decays for some intervals of time. It is hard to find a longer interval of a constant slope only for $E_0 = 1.5$ a.u. in the respective curve. In Fig. 5 we present the instantaneous ionization rate $\Gamma(t)$ as a function of time for four simulations [the same as in Fig. 4, but corresponding only to $E_0 = 1.5, 2, 3$, and 8 a.u.; $\Gamma(t)$ oscillates stronger for $E_0 = 13$ and 18 a.u., and

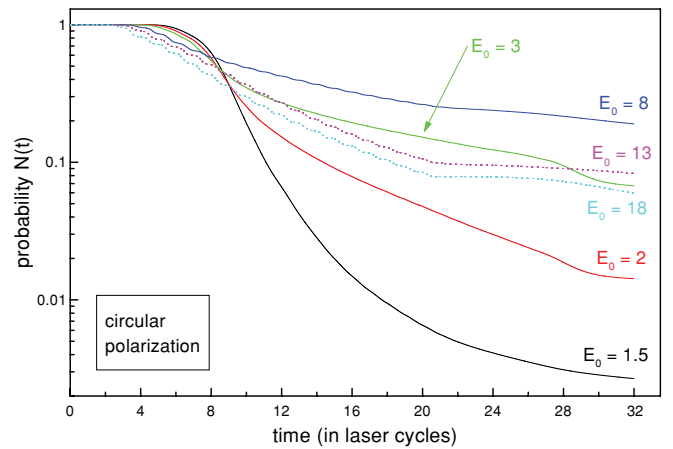


FIG. 4. (Color online) Probability $N(t)$ [Eq. (15a)] versus time for a trapezoidal circularly polarized laser pulse of the frequency $\omega = 1$ a.u.. The turn-on and turn-off times of the pulse are equal to four cycles. The flat part of the pulse is for $4 \leq t \leq 20$ (in laser cycles). There are six different values of the amplitude E_0 (as marked on the graph).

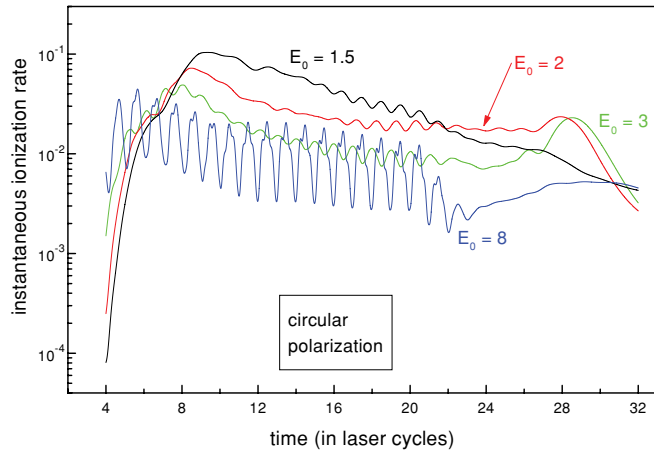


FIG. 5. (Color online) The instantaneous ionization rate [from Eq. (15), in a.u.] versus time for a trapezoidal circularly polarized laser pulse (the same as in Fig. 4). There are four different values of the amplitude E_0 (as marked on the graph).

the plot with these two lines would be illegible]. Taking into account an appearance of the curves from Figs. 4 and 5, we have decided to calculate average ionization rates in the time interval $12T \leq t \leq 20T$ (i.e., in the second half of the flat top of the laser pulse). Such a choice is justified also by the previously mentioned time delay in $\Gamma(t)$. This choice is, of course, arbitrary, and one could also extend the previously mentioned time interval beyond $t = 20T$ for some values of the peak field amplitude E_0 . The result of our calculations, made by the least-square method (at the confidence level of 95%), is given in Table II. Except for $E_0 = 8$ a.u., the data from Table II are roughly in agreement (up to a factor less than 2.5 at worst) with the data from Table I. The VG BSPM ionization rates (Γ_{VG}) are usually smaller than the gauge-invariant rates Γ , and the LG BSPM ionization rates (Γ_{LG}) are usually larger than Γ .

IV. REMARKS AND CONCLUSIONS

Geltman (in Ref. [11], p. 286) says that “. . . an ‘ionization rate’ is not a valid concept in the ultraintense limit. . .” In reality, only the instantaneous ionization rate may be well defined [see Eq. (11) or (15)]. However, at least for the circularly polarized and quite strong laser field, one can speak about the average ionization rate for the flat part of the pulse. Strictly speaking, this average rate depends not only on ω and

TABLE II. Gauge-invariant ionization rates [from the method (B)] for the circularly polarized laser field as a function of the electric field vector amplitude E_0 . The data have been obtained for the time interval $[12T, 20T]$ by the least-square method at the confidence level of 95%.

E_0 (a.u.)	Γ (a.u.)
1.5	$4.48 \pm 0.02[-2]$
2	$2.263 \pm 0.004[-2]$
3	$1.122 \pm 0.002[-2]$
8	$9.51 \pm 0.02[-3]$
13	$1.865 \pm 0.003[-2]$
18	$1.898 \pm 0.003[-2]$

TABLE III. The BSPM ionization rates (in both gauges) for the circularly polarized laser field as a function of the electric field vector amplitude E_0 . The data have been obtained with the help of random numbers (see text for more detail). Shown also is the ratio of both results.

E_0 (a.u.)	Γ_{VG} (a.u.)	Γ_{LG} (a.u.)	$\Gamma_{\text{LG}}/\Gamma_{\text{VG}}$
1.5	2.97[-2]	6.30[-2]	2.12
2	1.76[-2]	2.89[-2]	1.64
3	7.48[-3]	8.21[-3]	1.10
8	2.73[-4] ^a	1.37[-2]	–
13	1.02[-2]	3.28[-2]	3.22
18	1.24[-2]	3.89[-2]	3.14

^aIn the interval $[4T, 12T]$ $\Gamma_{\text{VG}} = -2.23[-3]$, and in the interval $[12T, 20T]$ $\Gamma_{\text{VG}} = 2.94[-3]$.

E_0 but on turn-on time of the pulse as well. But if the turn-on is slow enough, an evolution of the wave packet is approximately represented by a decay of a single Floquet state [17]. We leave studying such problems to a later paper, also with regard to strong-field theories and their predictive power with respect to a stabilization of the atom [5,6,11,13,16,17,20,21]. Our present work shows that usually the average ionization rate can change rather slowly during the flat part of the pulse. (This is not true for $E_0 = 8$ a.u. and the BSPM VG ionization rate, as discussed in the appendix.) Although our solution to the TDSE is numerically exact, all the ionization rates calculated by us are burdened with some uncertainty (which can be computed, e.g., by the least-square method).

In Sec. III we have mentioned two methods, which were often used to find (exact or approximate) ionization rates in non-perturbative laser fields. In Refs. [2,5,6,8–10,14,15,17,19–22] the method (A) was applied (and only in Ref. [16] the method (B) was applied), but in the references of Ref. [13] one can find several further examples. The method (A) (also called by us the BSPM) is used in perturbative laser fields as well. We have noted the discussion in Sec. 5 of Ref. [6]. According to Geltman, both methods are not equivalent and the author prefers the method (A) (in the LG) rather than the method (B). As revealed by our present numerical calculations, for the circularly polarized laser field, both methods of computing

TABLE IV. The BSPM ionization rates (in both gauges) for the circularly polarized laser field as a function of the electric field vector amplitude E_0 . The data have been obtained by the use of Eq. (13) for $t = 4T$ and $t = 20T$. Shown also is the ratio of both results.

E_0 (a.u.)	Γ_{VG} (a.u.)	Γ_{LG} (a.u.)	$\Gamma_{\text{LG}}/\Gamma_{\text{VG}}$
1.5	2.90[-2]	5.74[-2]	1.98
2	1.71[-2]	2.84[-2]	1.66
3	6.84[-3]	5.17[-3]	0.756
8	2.11[-3] ^a	7.47[-3]	–
13	1.07[-2]	2.71[-3]	0.253
18	7.72[-3]	3.38[-2]	4.38

^aIn the interval $[4T, 12T]$ $\Gamma_{\text{VG}} = 1.16[-3]$, and in the interval $[12T, 20T]$ $\Gamma_{\text{VG}} = 3.06[-3]$. Only for this method the ionization rate in the interval $[4T, 20T]$ is the arithmetic mean of ionization rates in the intervals $[4T, 12T]$ and $[12T, 20T]$.

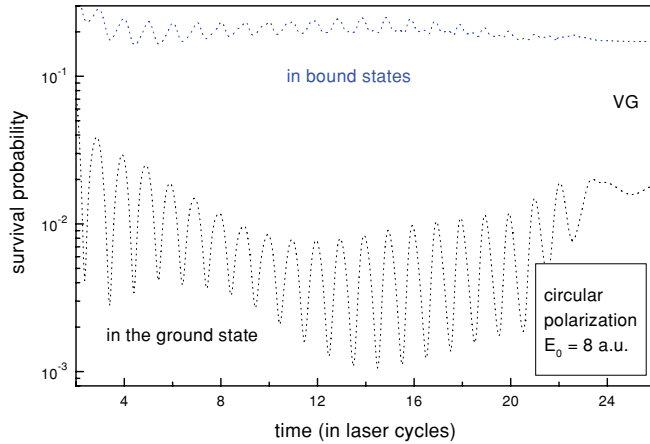


FIG. 6. (Color online) The same as for Fig. 2(d) (the circular polarization, $E_0 = 8$ a.u.), but without the LG survival probabilities. The VG survival probabilities are shown more exactly as a function of time, particularly for the flat top of the pulse [for $4 \leq t \leq 20$ (in laser cycles)].

ionization rates give different results, although of the same order of magnitude.

In conclusion, we have shown both analytically and numerically that strong-field photoionization rates, calculated for the flat part of the pulse by the method (A), may be quite markedly gauge dependent. The gauge-invariant method (B) gives values of the ionization rate lying between analogous values of the VG and the LG versions of method (A). For the circular polarization and the 2D model atom we have calculated numerically the BSPM ionization rates in both gauges (Γ_{LG} and Γ_{VG}) for several nonperturbative values of the electric peak field amplitude ($1.5 \text{ a.u.} \leq E_0 \leq 18 \text{ a.u.}$) and the laser frequency $\omega = 1 \text{ a.u.}$ Γ_{LG} is usually greater than Γ_{VG} and the ratio of the BSPM rates can reach a factor of 4. This fact points out that method (A) is not reliable in strong laser fields (at least for a quite high frequency like $\omega = 1 \text{ a.u.}$). For lower (optical or infrared) frequencies, the approximate S -matrix theory [based on method (A)] can produce satisfactory (also in an experimental context), but gauge-dependent ionization rates (see Refs. [8,22] and references therein). The difference between Γ_{LG} and Γ_{VG} vanishes in the limit of a weak laser field, as Eqs. (3), (8), and (9) clearly show. Although we have not used superstrong field parameters in our calculations, the present work suggests that for sufficiently strong fields divergences between Γ_{LG} and Γ_{VG} might grow with the field. This could be a certain explanation of divergences found before

by one of us (J.H.B.) in Refs. [8–10], and present in some other calculations of this type.

ACKNOWLEDGMENTS

We are indebted to Jarosław Zaremba for reading the manuscript and useful comments. One of us (J.H.B.) is also indebted to Sydney Geltman for calling the author's attention to Ref. [11] and to Piotr Kosiński for interesting discussions related to this work.

APPENDIX

In Sec. III (Table I) we have shown the BSPM ionization rates (in both gauges) obtained by the least-square method. Here we present the BSPM ionization rates for the same values of the peak electric field amplitude and circular polarization, but computed in a different way. All ionization rates presented in this work, which are defined by Eq. (11), are subject to some error. The error comes from the fact that (i) survival probabilities show rapid oscillations in time and (ii) Eq. (13) is valid only approximately even without oscillations. For the reason (i) we have not computed ionization rates for the linearly polarized field, where oscillations are huge. We do not give uncertainties of the ionization rates in Tables III and IV, because we treat these data only as estimate ones. In Table III there are ionization rates calculated by choosing randomly the point $t_0 \in [4T, 19T]$, taking $t_1 = t_0 + T$, and assuming the validity of Eq. (13) for both t_0 and t_1 . The numbers in Table III are the result of averaging over a very large number of shots (typically 10^7 or more), when the mean ionization rate becomes independent of the number of shots. (We have used two different random numbers generators and we have obtained identical results.) In Table IV there are the BSPM ionization rates calculated from Eq. (13) assuming that $t_0 = 4T$ and $t_1 = 20T$. In our opinion, the latter data are least credible, but we have given them for completeness. In Tables I, III, and IV the BSPM ionization rates in the VG for $E_0 = 8 \text{ a.u.}$ are marked by an upper index “a”. Figure 6 shows that, roughly speaking, the BSPM ionization rates for $t \in [4T, 12T]$ and for $t \in [12T, 20T]$ are different, and may even become negative. We do not see any physical reason for a negative ionization rate when the field is circularly polarized and the electric field vector amplitude is constant (in the flat part of the laser pulse). Therefore, there is a serious drawback of the BSPM VG ionization rates, revealed by numerical examples (for $E_0 = 8 \text{ a.u.}$) given in the present work. This is the fact that Γ_{VG} , unlike Γ_{LG} , can change significantly during the flat part of the pulse.

- [1] C. Cohen-Tannoudji, B. Diu, and F. Laloe, *Quantum Mechanics* (Hermann/Wiley, Paris, 1977).
- [2] D. H. Kobe and E. C. T. Wen, *Phys. Lett. A* **80**, 121 (1980).
- [3] M. H. Mittleman, *Introduction to the Theory of Laser-Atom Interactions* (Plenum Press, New York and London, 1982).
- [4] W. E. Lamb Jr., R. R. Schlicher, and M. O. Scully, *Phys. Rev. A* **36**, 2763 (1987).

- [5] R. Grobe and M. V. Fedorov, *J. Phys. B: At. Mol. Opt. Phys.* **26**, 1181 (1993).
- [6] S. Geltman, *J. Phys. B: At. Mol. Opt. Phys.* **27**, 257 (1994).
- [7] E. Cormier and P. Lambropoulos, *J. Phys. B: At. Mol. Opt. Phys.* **29**, 1667 (1996).
- [8] J. Bauer, *Phys. Rev. A* **73**, 023421 (2006).
- [9] J. H. Bauer, *Phys. Scr.* **77**, 015303 (2008); e-print arXiv:0706.2514v2 [physics.atom-ph].

- [10] J. H. Bauer, *J. Phys. B: At. Mol. Opt. Phys.* **41**, 185003 (2008).
- [11] S. Geltman, *Chem. Phys. Lett.* **237**, 286 (1995).
- [12] P. Lambropoulos, *Phys. Rev. Lett.* **55**, 2141 (1985).
- [13] M. Gavrilă, *J. Phys. B: At. Mol. Opt. Phys.* **35**, R147 (2002).
- [14] L. V. Keldysh, *Zh. Eksp. Teor. Fiz.* **47**, 1945 (1964) [*Sov. Phys. JETP* **20**, 1307 (1965)].
- [15] H. R. Reiss, *Phys. Rev. A* **22**, 1786 (1980).
- [16] D. Bauer and F. Ceccherini, *Phys. Rev. A* **66**, 053411 (2002).
- [17] M. Boca, H. G. Müller, and M. Gavrilă, *J. Phys. B: At. Mol. Opt. Phys.* **37**, 147 (2004).
- [18] R. Kosloff, *J. Phys. Chem.* **92**, 2087 (1988).
- [19] F. Robicheaux, C.-T. Chen, P. Gavras, and M. S. Pindzola, *J. Phys. B: At. Mol. Opt. Phys.* **28**, 3047 (1995).
- [20] R. Grobe and M. V. Fedorov, *Phys. Rev. Lett.* **68**, 2592 (1992).
- [21] M. Dondera, H. G. Müller, and M. Gavrilă, *Phys. Rev. A* **65**, 031405(R) (2002).
- [22] J. H. Bauer, *Phys. Rev. A* **75**, 045401 (2007).